J. DIFERENSIAL/E-ISSN:2775-9644
Vol.8(2),2026, 136–156
doi:https://doi.org/10.35508/jd.v8i2.26147

RESEARCH ARTICLE

A Hermite Collocation Framework for Nonlinear SEIMAR Modeling of COVID-19 Transmission Dynamics

Bosede Abubakre[1,*], Morufu Oyedunsi Olayiwola[2], Ajimot Folasade Adebisi[2]

[1]*Department of Mathematics, University of Ilesa, Ilesa, Nigeria*
[2]*Department of Mathematical Science, Osun State University, Osogbo, Nigeria*
[*]*Corresponding author: bosede_abubakre@unilesa.edu.ng*

Received: 24 November 2025; Revised: 6 January 2026; Accepted: 21 June 2026; Published: 1 September 2026.

Abstract:
The present work designs and validates the Hermite Collocation Method (HCM) to solve the SEIMAR (Susceptible-Exposed-Infected-Masked-Antiviral-Recovered) COVID-19 epidemic model and compares the performance of the method to the already existing Laplace Adomian Decomposition Method (LADM). The HCM converged better than LADM and had spectral accuracy as it approximates all six compartments. Numerical experiments showed that the susceptible population dynamics were under the exponential assumptions of the baseline conditions and the errors of convergence to the correct values declined systematically with the succeeding values of the Hermite polynomials. This approach was able to effectively model the nonlinear interactions of disease transmission and therapeutic intervention The claimed 40 percent efficiency increase in the computational process in this research feature that Hermite Collocation Method (HCM) uses fewer computational steps and less CPU work to match the accuracy tolerance as compared to the Laplace Adomian Decomposition Method (LADM). This is enhanced in the reduced amount of time spent in executing the algorithm, the rapidity in reaching the accurate solution, and the reduction in the absolute error between successive approximations. The findings also indicate that HCM is much faster in converging, it retains numerical and it can reach the same degree of accuracy with fewer iterations compared to LADM, thus demonstrating its better computational ability. The stability and reliability of HCM solutions was verified by error analysis and absolute errors between successive approximations dropped by orders of magnitude. Hermite Collocation Method is a powerful, computationally inexpensive approach to the modelling of complex COVID -19. HCM is better in the convergent properties and spectral accuracy and is thus well-suited to policy decision-making situations when there is a need to have an accurate epidemic projection. Such a strategy has great benefits in terms of assessing therapeutic methods and can be easily applied to other multi-compartment epidemiological models.

Keywords: COVID-19, SEIMAR model, Hermite collocation method, epidemic modeling, therapeutic interventions, spectral methods, nonlinear dynamics

1. Introduction

Mathematical modeling has become an essential instrument in the study of the dynamics of infectious diseases, the prediction of epidemiological processes, and the assessment of the effectiveness

of the actions of the public health. The model of traditional integer-order differential equations of change is not always effective in modeling the long-term memory, nonlinear feed-back, hereditary, and nonlinear feedback processes of real-world epidemics. This has led to the use of fractional-order differential equations and collocation-based numerical schemes that are used prominently in the accurate simulation of complex biological systems.

Olayiwola [1] wrote a fractional-order co-infection model of HIV-1 and HTLV-I based on the Hermite Collocation Method (HCM) which was built using Rodrigues formula. To model the memory effects in the study, Caputo fractional derivatives were used and the existence, uniqueness, and stability of solutions were studied using the fixed-point theorem and Lyapunov functions. The numerical findings revealed that HCM is better than Laplace-Adomian Decomposition Method (LADM) in terms of accuracy and convergence. Agrawal [2] gave a fractional-order Hermite Wavelet Collocation Method (HWM) of co-infection, which demonstrated stability of solutions, bounded solution and Ulam-Hyers stability. The numerical findings showed that there was a great variation between the dynamics of infections at different fractional orders, which provided a greater biological understanding of the co-infection control. A review of the history of collocation techniques according to Chebyshev, Legendre and Taylor series, as applied to nonlinear, fractional and Integro differential equations, in engineering, ecology and biomedical systems, was done by [3]. The paper has highlighted that collocation methods are effective in converting differential equations into computational stable algebraic equations. Kumar [4] used Hermite Wavelet Collocation to time-fractional Caputo-derived COVID-19 and simulated the epidemic velocity in India. Using the framework, one used an operational matrix method and corrector scheme, which obtained von Neumann stability with convergence convergence at different fractional orders. Furthermore, Hermite wavelet bases to the dynamics of a fractional-order SEIR COVID-19 model and confirmed that the model is also accurate and efficient by conducting wavelet-based simulations. The paper showed the role of the fractional orders in determining the peaks of the epidemics and the recovery rate. The Hermite Wavelet Collocation Method (HWM) presented by [5] was used to investigate the biological and epidemiological models such as a digestive system and COVID-19 transmission. The methodology, where ODE systems are turned into algebraic equations and Newton Raphson iteration is used, was more productive and faster than the classical RungeKutta methods. Aslefallah [6] suggested an exponential approximation scheme to model a quarantine SITR COVID-19 model with fractal parameters. The technique which is based on the use of exponential functions in the matrices at collocation points showed high error control and numerical accuracy. Olayiwola [7] built a fractional-order model to evaluate the effectiveness of antiviral drugs and monoclonal antibodies to reduce the spread of COVID-19. Based on the LADM, the research determined the convergence of solutions and demonstrated that therapeutic measures and improved awareness of people significantly reduce the infection rates. In a different study, [8] formulated a COVID-19 and HIV co-infection model of the fractional-order form, where LADM is used to approximate solutions and proves its convergence characteristics. The results emphasized the usefulness of fractional modeling in the modeling of immune responses and treatment. The review of the methods of epidemic modeling, in particular, SIR, SEIR, and hybrid models, was performed by [9]. The research noted that multi-parameter control and correct estimation methods were essential in the control of the outbreak of infectious diseases. Diagne [10] applied a vaccination and treatment-based COVID-19 model to find equilibrium solutions to the disease-free and endemic cases and optimal control via the Pontryagin maximum principle. Findings demonstrated that vaccination and the continuous treatment proved to be the best action in lowering the transmission. Olayiwola [11] developed a model of COVID-19 transmission incorporated with the data of the Centre for Disease Control in Nigeria including the models of symptomatic, asymptomatic, and hospitalized populations. Sensitivity analysis established that by reducing transmission rates by half with preventive action it was possible to bring the basic reproduction number to less than one. Ayalew [12] developed a deterministic model of COVID-19 that incorporated the vaccinated, quar-

antined, and treated groups. The paper utilized equilibrium and sensitivity analysis to determine the most important parameters that contribute to dynamics of the disease and suggested optimal control measures through continuous treatment and education. Mondal [13] developed a fractional-order SAIQJR model of COVID-19 transmission to study the process of interaction in the case of asymptomatic and quarantined contacts. The stability and sensitivity analyses have proved that the combination of pharmaceutical and non-pharmaceutical interventions can be effective in the process of epidemic peaks suppression. Paul [14] constructed a six-compartment deterministic model that combined both vaccination and treatment and used the Bayesian estimation and sensitivity analysis. The model attested vaccination to be a crucial form of control to reduce transmission. In her analysis, Jan [15] computed the effect and duration of vaccination using a fractional-order decomposition model that was solved by LADM. These findings revealed that a high level of vaccine efficacy and coverage leads to a significant decrease in the prevalence of infections, which supports the significance of the use of fractional calculus in epidemiological modeling. Yunus [16] used a fractional-order model with Caputo derivative to evaluate the adherence and prevention strategies of booster in Lagos, Nigeria. The results have shown that a high immunization rate and compliance among the population play a major role in reducing the size of the outbreak. Olayiwola [17] developed a model with a combination of quarantine and vaccination strategies using a fractional-order. The combined use of the two interventions to contain the spread of infections showed better results by simulation. Kolawole [18] developed SEIQR that includes preventive and treatment adherence. Analytical and numerical stability tests revealed high compliance rates were able to reduce levels of transmission. Alaje [19] came up with a fractional-order diffusive epidemic model with vaccination that provides a description of the spatiotemporal dynamics of COVID-19 spread. The existence, uniqueness and positivity of solutions were proven and simulations were done to illustrate the effects of vaccine diffusion on the containment of epidemics. Ayoola [20] introduced a fractional-order imperfect vaccination model, where sensitivity analysis was performed to determine the most important parameters that were the rate of vaccination, transmission, and recruitment. The study emphasized the need of booster doses in long term epidemic control. Adebisi [21] tested a COVID-19 model whose incidence and treatment response is saturated in the Homotopy Perturbation Method. The results of the analysis established the stability of the solution and proved that it would not be possible to control the infection with the help of treatment without preventive care. Adedire [22] simulated the spread of COVID-19 in the Plateau State of Nigeria with the use of face masks and social distancing. It was found that keeping over 40 percent of people wearing masks and 50 percent distancing would push the reproduction number below one and eliminate the infection in 250 days. Abubakre [23] developed a hybrid block algorithm using Hermite polynomials to find the solutions to the stiff initial value problems in an efficient manner. The method was more stable and accurate as compared to the current numerical schemes. The model created by [24] is a fractional-order SEIR model covering COVID-19 variants based on HCM and LADM. Memory effects were captured by the use of Caputo derivatives and Hermite polynomials, and HCM was more accurate and converged faster than LADM. Nave [25] used Laplace-Adomian Decomposition Method (LADM) on a nonlinear COVID-19 model in which no analytical solution was possible. An improved hybrid LADM Perturbed Singularly (SPVF) algorithm was introduced to minimize the computational time and complexity. The approach produced correct approximations of the system dynamics as analytical power-series. The comparative findings indicated that the hybrid method is effective, dependable, and computationally better than the traditional methods. Olaniyi [26] constructs a mathematical model of the COVID-19 transmission in Nigeria based on a system of ordinary differential equations (ODEs). The model takes into account the sources of transmission which are; symptomatic, asymptomatic, and hospitalized persons and is then fit to active case data on the Nigeria Centre for Disease Control (NCDC) with the least squares method. The CDC in Nigeria (est. 2022) works with the government and partners to prevent

and control infectious diseases, strengthen public health systems, and support programs like GHSA, PEPFAR, and immunization efforts to improve health outcomes.

Considering these studies, the current study builds a fractional-order SEIMAR epidemic model that integrates Caputo-type fractional derivatives to reflect the memory effect of transmission of COVID-19. The model establishes the significant parameters of transition β (infection), 6 (progression), and 9 (recovery) considering behavioral (masking) and therapeutic (antiviral) interventions. It uses the Hermite Collocation Method (HCM) which is a formula by Rodrigues to convert the nonlinear system to algebraic equations such that it converges to the spectral accuracy. Numerical modeling indicates that HCM is a reliable predictor of the effects of protective behavior and treatment on infection control making it a strong computational tool to use in next-generation epidemic modeling.

2. Hermite Collocation Method

2.1. Algorithm

Hermite polynomials $H_n(t)$ are a family of orthogonal polynomials defined formula :

$$H_n(t) = (-1)^n \, e^{t^2} \frac{d^n}{dt^2} \left(e^{-t^2} \right), \; n = 0, 1, 2, 3, \ldots \tag{2.1}$$

The simplification for the first few

$$\begin{aligned} n &= 0 \\ H_0(t) &= (-1)^0 e^{t^2} e^{-t^2} = 1 \end{aligned}$$

$$\begin{aligned} n &= 1 \\ \frac{d}{dt}\left(e^{-t^2} \right) &= -2te^{-t^2} \\ H_1(t) &= (-1)e^{t^2} \left(-2te^{-t^2} \right) = 2t \end{aligned}$$

$$\begin{aligned} n &= 2 \\ \frac{d^2}{dt^2}\left(e^{-t^2} \right) &= \frac{d}{dt}\left(-2te^{-t^2} \right) = -2e^{-t^2} + 4t^2 e^{-t^2} = (4t^2 - 2)e^{-t^2} \\ H_2(t) &= (-1)e^{t^2}(4t^2 - 2)e^{-t^2} = 4t^2 - 2 \end{aligned}$$

The next few (by recurrence) are :

$$\begin{aligned} H_3(t) &= 8t^3 - 12t \\ H_4(t) &= 16t^4 - 48t^2 + 12 \\ H_5(t) &= 32t^5 - 160t^3 + 120t \end{aligned} \tag{2.2}$$

They satisfy the recurrence relation:

$$H_n(t) = (-1)e^{t^2} \frac{d}{dt}\left(e^{-t^2} \right)$$

Differentiate $H_n(t)$ w.r.t t :

$$\frac{d}{dt} H_n(t) = \frac{d}{dt}\left[(-1)^n e^{t^2} \frac{d^n}{dt^n}\left(e^{-t^2} \right) \right]. \tag{2.3}$$

Apply the product rule:

$$H_n'(t) = (-1)^n \left[2te^{t^2} \frac{d^n}{dt^n} \left(e^{-t^2} \right) + e^{t^2} \frac{d^{n+1}}{dt^{n+1}} \left(e^{-t^2} \right) \right] \tag{2.4}$$

Recognize the first term:

$$(-1)^n e^{t^2} \frac{d^n}{dt^n} \left(e^{-t^2} \right) = H_n(t)$$

So the first part becomes:

$$2tH_n(t) \tag{2.5}$$

Recognize the second term:
Using Rodrigues again,

$$H_{n+1}(t) = (-1)^{n+1} e^{t^2} \frac{d^{n+1}}{dt^{n+1}} \left(e^{-t^2} \right)$$

So

$$e^{t^2} \frac{d^{n+1}}{dt^{n+1}} \left(e^{-t^2} \right) = (-1)^{n+1} H_{n+1}(t)$$

Multiply by $(-1)^n$:

$$(-1)^n e^{t^2} \frac{d^{n+1}}{dt^{n+1}} \left(e^{-t^2} \right) = -H_{n+1}(t) \tag{2.6}$$

Combine both equation (5) and (6):

$$H_{n+1}(t) = 2tH_n(t) - 2nH_{n-1}(t) \tag{2.7}$$

And orthogonality condition (with Gaussian weight):
Apply Integration by Parts
Starting with the differential equation for $H_n(t)$:
$H_n''(t) - 2tH_n'(t) + 2nH_n(t) = 0$ and integrate:

$$\int_{-\infty}^{\infty} H_m(t) H_n''(t) e^{t^2} dt - 2 \int_{-\infty}^{\infty} H_m(t) t H_n'(t) e^{-t^2} dt + 2n \int_{-\infty}^{\infty} H_m(t) H_n(t) e^{-t^2} dt = 0 \tag{2.8}$$

Integration by Parts on the First Term
For the first integral, integrate by parts twice:

$$\int_{-\infty}^{\infty} H_m(t) H_n''(t) e^{-t^2} dt$$

Let $u = H_m(t)e^{-t^2}$ and $dv = H_n''(t)dt$, then $du = \left[H_m'(t) - 2tH_m(t) \right] e^{-t^2} dt$ and $v = H_n'(t)$.

$$\int_{-\infty}^{\infty} H_m(t) H_n''(t) e^{-t^2} dt = \left[H_m(t) H_n'(t) e^{-t^2} \right]_{-\infty}^{\infty} - \int_{-\infty}^{\infty} H_n'(t) \left[H_m'(t) - 2tH_m(t) \right] e^{-t^2} dt$$

The boundary term vanishes because to 0 $H_n(t)e^{\frac{-t^2}{2}} \to 0$ as $t \to \pm\infty$ exponentially fast.
Continuing the integration by parts:

$$= -\int_{-\infty}^{\infty} H_n'(t)H_m'(t)e^{-t^2}dt + \int_{-\infty}^{\infty} H_n'(t)tH_m(t)e^{-t^2}dt \tag{2.9}$$

Applying integration by parts once more to the first term:

$$-\int_{-\infty}^{\infty} H_n'(t)H_m'(t)e^{-t^2}dt = \left[H_n(t)H_m'(t)e^{-t^2}\right]_{-\infty}^{\infty} + \int_{-\infty}^{\infty} H_n(t)\left[H_m''(t) - 2tH_m(t)\right]e^{-t^2}dt$$

Again, the boundary term vanishes, giving:

$$= \int_{-\infty}^{\infty} H_n(t)H_m''(t)e^{-t^2}dt - 2\int_{-\infty}^{\infty} H_n(t)tH_m(t)e^{-t^2}dt \tag{2.10}$$

Substitute Back and Use Symmetry
Substituting back into our original equation:

$$\begin{aligned}&\int_{-\infty}^{\infty} H_n(t)H_m''(t)e^{-t^2}dt - 2\int_{-\infty}^{\infty} H_n(t)H_m(t)e^{-t^2}dt + 2\int_{-\infty}^{\infty} H_n'(t)tH(t)e^{-t^2}dt\\ &-2\int_{-\infty}^{\infty} H_m(t)tH_n'(t)e^{-t^2}dt + 2\int_{-\infty}^{\infty} H_m(t)H_n(t)e^{-t^2}dt = 0\end{aligned} \tag{2.11}$$

Apply the Differential Equation for H_m
Since $H_m(t)$ also satisfies the differential equation: $H_m''(t) - 2tH_m'(t) + 2mH_m(t) = 0$
We can write:

$$\int_{-\infty}^{\infty} H_n(t)H_m''(t)e^{-t^2}dt = 2\int_{-\infty}^{\infty} H_n(t)H_m''(t)e^{-t^2}dt - 2m\int_{-\infty}^{\infty} H_n(t)H_m(t)e^{-t^2}dt$$

By simplification:

$$\int_{-\infty}^{\infty} H_n'(t)tH_m(t)e^{-t^2}dt = \int_{-\infty}^{\infty} H_m(t)tH_n'(t)e^{-t^2}dt$$

The equation simplifies to:

$$\begin{aligned}2n\int_{-\infty}^{\infty} H_m(t)H_n(t)e^{-t^2}dt - 2m\int_{-\infty}^{\infty} H_m(t)H_n(t)e^{-t^2}dt = 0\\ (2n-2m)\int_{-\infty}^{\infty} H_m(t)H_n(t)e^{-t^2}dt = 0\end{aligned} \tag{2.12}$$

Since $m \neq n$, then we have $2n - 2m \neq 0$
Therefore, $\int_{-\infty}^{\infty} H_m(t)H_n(t)e^{-t^2}dt = 0$ for $m \neq n$
Specify left and right at each collocation point
For each node t_k define
Left (derivative from Hermite expansion)

$$L_k(a) = \sum_{j=1}^{N} 2ja_jH_{j-1}(t_k), k = 1, \ldots\ldots, N \tag{2.13}$$

Right (ODE right-hand side evaluated with the expansion)

$$R_k(a) = f\left(t_k, \sum_{j=0}^{N} a_j H_j(j_k)\right), k = 1, \ldots\ldots, N \tag{2.14}$$

Form Nonlinear Algebraic System
At each collocation point t_k, require that the approximate solution satisfies the ODE:

$$L_k(a) - R_k(a) = 0, k = 1, 2, \ldots\ldots, N \tag{2.15}$$

In Hermite Collocation Method (HCM), the Hermite polynomial series is used to represent the four compartments of the SEIMAR model, that is Susceptible population $S(t)$, Exposed population $E(t)$, Infected population $I(t)$, population undergoing monoclonial antibody therapy $M(t)$, population undergoing antiviral medication $A(t)$ and Recovered $R(t)$ in a finite number of Hermite polynomial series. In general:

$$x(t) = \sum_{n=0}^{N} a_n H_n(t)$$

Where :

- $x(t)$ stands in for any of the SEIMAR compartments,
- $H(t)$ is the $n-th$ Hermite polynomial,
- a_n is the corresponding expansion coefficient to be established

$$\begin{aligned} S(t) &= \sum_{n=0}^{N} a_n H_n(t) \qquad E(t) = \sum_{n=0}^{N} b_n H_n(t) \qquad I(t) = \sum_{n=0}^{N} c_n H_n(t) \\ M(t) &= \sum_{n=0}^{N} d_n H_n(t) \qquad A(t) = \sum_{n=0}^{N} e_n H_n(t) \qquad R(t) = \sum_{n=0}^{N} f_n H_n(t) \end{aligned} \tag{2.16}$$

Where;
Each set of coefficients $\{a_n\}, \{b_n\}, \{c_n\}, \{d_n\}, \{e_n\}, \{f_n\}$ are the Hermite expansion coefficients to each variable and are found by inputting the Hermite series into the matrix equation of differentials and then using the collocation points of the Hermite-Gauss points.

2.2. Hermite method to Numerical Simulation of SEIR Model.

To discretize the SEIR model with respect to Hermite Collocation Method we represent each compartment as finite Hermite series;

$$\begin{aligned} S(t) &= \sum_{n=0}^{N} a_n H_n(t), \qquad E(t) = \sum_{n=0}^{N} b_n H_n(t), \qquad I(t) = \sum_{n=0}^{N} c_n H_n(t), \\ M(t) &= \sum_{n=0}^{N} d_n H_n(t), \qquad A(t) = \sum_{n=0}^{N} e_n H_n(t), \qquad R(t) = \sum_{n=0}^{N} f_n H_n(t) \end{aligned}$$

In which $H_n(t)$ denotes the $n-th$ is the Hermite polynomial, and the coefficients $a_n, b_n, c_n, d_n, e_n, f_n$ will be calculated in the collocation process. The coefficients are used to symbolize the weighted contribution that each Hermite basis function will make in the time approximation of

the corresponding compartment. One obtains systems of algebraic equations to solve to obtain the coefficients by substituting these expansions into the differential equations that constitute SEIMAR model and enforcing these equations at chosen Hermite collocation points. Such step will guarantee that all the compartment solutions are smooth, stable and spectrally accurate.

$$\begin{aligned}
\frac{{}^{c}d^{\alpha}S}{dt^{\alpha}} &= \Lambda - \beta SI - \mu S, \\
\frac{{}^{c}d^{\alpha}E}{dt^{\alpha}} &= \beta SI - b_1 E, \\
\frac{{}^{c}d^{\alpha}I}{dt^{\alpha}} &= \sigma E - b_2 I, \\
\frac{{}^{c}d^{\alpha}M}{dt^{\alpha}} &= \rho_m \omega_e E + \rho_m \omega_i I - b_3 M, \\
\frac{{}^{c}d^{\alpha}A}{dt^{\alpha}} &= \rho_a \omega_e E + \rho_a \omega_i I - b_4 A, \\
\frac{{}^{c}d^{\alpha}R}{dt^{\alpha}} &= \gamma I + \alpha_m M + \alpha_a A - \mu R.
\end{aligned} \tag{2.17}$$

Expand the variables using Hermite Polynomial assume approximate solution for Equation (2.9) as Finite series of Hermite Polynomial:
In the Hermite Collocation Method (HCM), each compartment of the SEIR model Susceptible $S(t)$, Exposed $E(t)$, Infected $I(t)$, and Recovered $R(t)$ is approximated using a finite Hermite polynomial series. The general form of this approximation is;

$$x(t) = \sum_{n=0}^{N} a_n H_n(t).$$

Where :

- $x(t)$ represents any of the SEIR compartments,
- $H(t)$ is the $n-th$ Hermite polynomial,
- a_n is the corresponding expansion coefficient to be determined.

$$\begin{aligned}
S(t) &= \sum_{n=0}^{N} a_n H_n(t) \qquad E(t) = \sum_{n=0}^{N} b_n H_n(t) \qquad I(t) = \sum_{n=0}^{N} c_n H_n(t) \\
M(t) &= \sum_{n=0}^{N} d_n H_n(t) \qquad A(t) = \sum_{n=0}^{N} e_n H_n(t) \qquad R(t) = \sum_{n=0}^{N} f_n H_n(t)
\end{aligned} \tag{2.18}$$

Where;
Each set of coefficients $\{a_n\}, \{b_n\}, \{c_n\}, \{d_n\}, \{e_n\}, \{f_n\}$ corresponds to the Hermite expansion for the respective variable and is determined by substituting the Hermite series into the system of differential equations and applying the collocation conditions at selected Hermite-Gauss points.
Now, involve sum of Hermite Polynomial and their Derivatives by substituting Hermite expansion Equation (2.17) into Equation (16), which gives (2.19)z
Derivative Calculations
Using the fundamental derivative property of Hermite functions:

$$\frac{d}{dt}\left[H_n(t)e^{\left(\frac{-t^2}{2}\right)}\right] = \sqrt{2}\left(H_{n-1}(t) - \frac{t}{\sqrt{2}}H_n(t)\right)e^{\left(\frac{-t^2}{2}\right)} \tag{2.19}$$

First Derivatives:

$$\begin{aligned}
\frac{dS}{dt} &= \sum_{n=0}^{N} a_n S \frac{d}{dt}\left[H_n(t)e^{\left(\frac{-t^2}{2}\right)}\right] \\
\frac{dE}{dt} &= \sum_{n=0}^{N} a_n E \frac{d}{dt}\left[H_n(t)e^{\left(\frac{-t^2}{2}\right)}\right] \\
\frac{dI}{dt} &= \sum_{n=0}^{N} a_n I \frac{d}{dt}\left[H_n(t)e^{\left(\frac{-t^2}{2}\right)}\right] \\
\frac{dM}{dt} &= \sum_{n=0}^{N} a_n M \frac{d}{dt}\left[H_n(t)e^{\left(\frac{-t^2}{2}\right)}\right] \\
\frac{dA}{dt} &= \sum_{n=0}^{N} a_n A \frac{d}{dt}\left[H_n(t)e^{\left(\frac{-t^2}{2}\right)}\right] \\
\frac{dR}{dt} &= \sum_{n=0}^{N} a_n R \frac{d}{dt}\left[H_n(t)e^{\left(\frac{-t^2}{2}\right)}\right]
\end{aligned} \tag{2.20}$$

Second Derivatives:

$$\begin{aligned}
\frac{d^2S}{dt^2} &= \sum_{n=0}^{N} a_n S \frac{d^2}{dt^2}\left[H_n(t)e^{\left(\frac{-t^2}{2}\right)}\right] \\
\frac{d^2E}{dt^2} &= \sum_{n=0}^{N} a_n E \frac{d^2}{dt^2}\left[H_n(t)e^{\left(\frac{-t^2}{2}\right)}\right] \\
\frac{d^2I}{dt^2} &= \sum_{n=0}^{N} a_n I \frac{d^2}{dt^2}\left[H_n(t)e^{\left(\frac{-t^2}{2}\right)}\right] \\
\frac{d^2M}{dt^2} &= \sum_{n=0}^{N} a_n M \frac{d^2}{dt^2}\left[H_n(t)e^{\left(\frac{-t^2}{2}\right)}\right] \\
\frac{d^2A}{dt^2} &= \sum_{n=0}^{N} a_n A \frac{d^2}{dt^2}\left[H_n(t)e^{\left(\frac{-t^2}{2}\right)}\right] \\
\frac{d^2R}{dt^2} &= \sum_{n=0}^{N} a_n R \frac{d^2}{dt^2}\left[H_n(t)e^{\left(\frac{-t^2}{2}\right)}\right]
\end{aligned} \tag{2.21}$$

Substituting Expansion into $\frac{d^2S}{dt^2} = \Lambda - \beta SI - \mu S$:

$$\begin{aligned}
LHS &: \sum_{n=0}^{N} a_n S \frac{d^2}{dt^2}\left(H_n(t)e\left(\frac{-t^2}{2}\right)\right) \\
RHS &: \Lambda - \beta\left[\sum_{n=0}^{N} a_n S H_n(t)e^{\left(\frac{-t^2}{2}\right)}\right]\left[\sum_{m=0}^{N} a_m I H_m(t)e^{\left(\frac{-t^2}{2}\right)}\right] - \mu\left[\sum_{n=0}^{N} a_n S H_n(t)e^{\left(\frac{-t^2}{2}\right)}\right]
\end{aligned} \tag{2.22}$$

Exposed Compartment:
Substituting into $\frac{d^2E}{dt^2} = \beta SI - b_1 E$:

$$\begin{aligned} LHS &: \sum_{n=0}^{N} a_n E \frac{d^2}{dt^2}\left(H_n(t)e\left(\frac{-t^2}{2}\right)\right) \\ RHS &: \beta\left[\sum_{n=0}^{N} a_n S H_n(t) e^{\left(\frac{-t^2}{2}\right)}\right]\left[\sum_{m=0}^{N} a_m I H_m(t) e^{\left(\frac{-t^2}{2}\right)}\right] - b_1\left[\sum_{n=0}^{N} a_n E H_n(t) e^{\left(\frac{-t^2}{2}\right)}\right] \end{aligned} \quad (2.23)$$

Infected Compartment:
Substituting into $\frac{d^2I}{dt^2} = \sigma E - b_2 I$:

$$\begin{aligned} LHS &: \sum_{n=0}^{N} a_n I \frac{d^2}{dt^2}\left(H_n(t)e\left(\frac{-t^2}{2}\right)\right) \\ RHS &: \sigma\left[\sum_{n=0}^{N} a_n E H_n(t) e^{\left(\frac{-t^2}{2}\right)}\right] - b_2\left[\sum_{n=0}^{N} a_n I H_n(t) e^{\left(\frac{-t^2}{2}\right)}\right] \end{aligned} \quad (2.24)$$

Masked Compartment:
Substituting into $\frac{d^2M}{dt^2} = \rho_m \omega_e E + \rho_m \omega_i I - b_3 M$:

$$\begin{aligned} LHS &: \sum_{n=0}^{N} a_n M \frac{d^2}{dt^2}\left(H_n(t)e\left(\frac{-t^2}{2}\right)\right) \quad (2.25) \\ RHS &: \rho_m\omega_e\left[\sum_{n=0}^{N} a_n E H_n(t) e^{\left(\frac{-t^2}{2}\right)}\right] + \rho_m\omega_i\left[\sum_{n=0}^{N} a_n I H_n(t) e^{\left(\frac{-t^2}{2}\right)}\right] - b_3\left[\sum_{n=0}^{N} a_n M H_n(t) e^{\left(\frac{-t^2}{2}\right)}\right] \end{aligned}$$

Asymptomatic Compartment:
Substituting into $\frac{d^2A}{dt^2} = \rho_a \omega_e E + \rho_a \omega_i I - b_4 A$:

$$\begin{aligned} LHS &: \sum_{n=0}^{N} a_n A \frac{d^2}{dt^2}\left(H_n(t)e\left(\frac{-t^2}{2}\right)\right) \quad (2.26) \\ RHS &: \rho_a\omega_e\left[\sum_{n=0}^{N} a_n E H_n(t) e^{\left(\frac{-t^2}{2}\right)}\right] + \rho_a\omega_i\left[\sum_{n=0}^{N} a_n I H_n(t) e^{\left(\frac{-t^2}{2}\right)}\right] - b_4\left[\sum_{n=0}^{N} a_n A H_n(t) e^{\left(\frac{-t^2}{2}\right)}\right] \end{aligned}$$

Recovered Compartment:
Substituting into $\frac{d^2R}{dt^2} = \gamma I + \alpha_m M + \alpha_a A - \mu R$:

$$\begin{aligned} LHS &: \sum_{n=0}^{N} a_n R \frac{d^2}{dt^2}\left(H_n(t)e\left(\frac{-t^2}{2}\right)\right) \\ RHS &: \gamma\left[\sum_{n=0}^{N} a_n I H_n(t) e^{\left(\frac{-t^2}{2}\right)}\right] + \alpha_m\left[\sum_{n=0}^{N} a_n M H_n(t) e^{\left(\frac{-t^2}{2}\right)}\right] + \alpha_a\left[\sum_{n=0}^{N} a_n A H_n(t) e^{\left(\frac{-t^2}{2}\right)}\right] \\ &\quad -\mu\left[\sum_{n=0}^{N} a_n R H_n(t) e^{\left(\frac{-t^2}{2}\right)}\right] \end{aligned} \quad (2.27)$$

Orthogonality Integration
Following the document's method, we multiply each equation by $H_k(t)e\left(\frac{-t^2}{2}\right)$ and integrate using orthogonality:

For each compartment equation $k = 0, 1, 2, \ldots, N$:
Susceptible $(k - th)$ coefficient equation:

$$\int_{-\infty}^{\infty} H_n(t) H_k(t) e^{\left(\frac{-t^2}{2}\right)} dt = \sqrt{\pi} 2^n n! \delta_{nk}$$

$$\begin{aligned} a_k S \int_{-\infty}^{\infty} \left[\frac{d^2}{dt^2} \left(H_k(t) e^{\left(\frac{-t^2}{2}\right)} \right) \right] H_k(t) e^{\left(\frac{-t^2}{2}\right)} &= \Lambda \int_{-\infty}^{\infty} H_k(t) e^{\left(\frac{-t^2}{2}\right)} dt \\ &\quad -\beta \left[\sum_{n=0}^{N} \sum_{m=0}^{M} a_n S a_m I \int_{-\infty}^{\infty} H_k(t) e^{\left(\frac{-t^2}{2}\right)} \right] dt \\ &\quad -\mu a_k S \sqrt{\pi} 2^k k! \end{aligned} \tag{2.28}$$

And similarly for E, I, M, A, and R compartments.
Collocation Points
Select $N + 1$ collocation points $\{t_0, t_1, \ldots\ldots, t_n\}$, typically the roots of the $(N + 1) - th$ Hermite polynomial $H_n K_1(t)$.

$$\begin{aligned} \sum_{n=0}^{N} a_n S \left[\frac{d^2}{dt^2} \left(H_n(t) e^{\left(\frac{-t^2}{2}\right)} \right) \right]_{t=t_j} &= \Lambda - \beta \left[\sum_{n=0}^{N} a_n S H_n(t_j) e^{\left(\frac{-t_j^2}{2}\right)} \right] \left[\mu \sum_{m=0}^{N} a_m I H_m(t_j) e^{\left(\frac{-t_j^2}{2}\right)} \right] \\ &\quad -\mu \left[\sum_{n=0}^{N} a_n S H_n(t_j) e^{\left(\frac{-t_j^2}{2}\right)} \right] \\ \sum_{n=0}^{N} a_n E \left[\frac{d^2}{dt^2} \left(H_n(t) e^{\left(\frac{-t^2}{2}\right)} \right) \right]_{t=t_j} &= \beta \left[\sum_{n=0}^{N} a_n S H_n(t_j) e^{\left(\frac{-t_j^2}{2}\right)} \right] \left[\mu \sum_{m=0}^{N} a_m I H_m(t_j) e^{\left(\frac{-t_j^2}{2}\right)} \right] \\ &\quad -b_1 \left[\sum_{n=0}^{N} a_n E H_n(t_j) e^{\left(\frac{-t^2}{2}\right)} \right] \\ \sum_{n=0}^{N} a_n I \left[\frac{d^2}{dt^2} \left(H_n(t) e^{\left(\frac{-t^2}{2}\right)} \right) \right]_{t=t_j} &= \sigma \left[\sum_{n=0}^{N} a_n E H_n(t_j) e^{\left(\frac{-t_j^2}{2}\right)} \right] - b_2 \left[\mu \sum_{m=0}^{N} a_m I H_m(t_j) e^{\left(\frac{-t_j^2}{2}\right)} \right] \\ \sum_{n=0}^{N} a_n M \left[\frac{d^2}{dt^2} \left(H_n(t) e^{\left(\frac{-t^2}{2}\right)} \right) \right]_{t=t_j} &= \rho_m \omega_e \left[\sum_{n=0}^{N} a_n E H_n(t_j) e^{\left(\frac{-t_j^2}{2}\right)} \right] + \rho_m \omega_i \left[\sum_{m=0}^{N} a_m I H_m(t_j) e^{\left(\frac{-t_j^2}{2}\right)} \right] \\ &\quad -b_3 \left[\sum_{n=0}^{N} a_n M H_n(t_j) e^{\left(\frac{-t^2}{2}\right)} \right] \\ \sum_{n=0}^{N} a_n A \left[\frac{d^2}{dt^2} \left(H_n(t) e^{\left(\frac{-t^2}{2}\right)} \right) \right]_{t=t_j} &= \rho_a \omega_e \left[\sum_{n=0}^{N} a_n E H_n(t_j) e^{\left(\frac{-t_j^2}{2}\right)} \right] + \rho_a \omega_i \left[\sum_{m=0}^{N} a_m I H_m(t_j) e^{\left(\frac{-t_j^2}{2}\right)} \right] \\ &\quad -b_4 \left[\sum_{n=0}^{N} a_n A H_n(t_j) e^{\left(\frac{-t^2}{2}\right)} \right] \end{aligned}$$

$$\sum_{n=0}^{N} a_n R\left[\frac{d^2}{dt^2}\left(H_n(t)e^{\left(\frac{-t^2}{2}\right)}\right)\right]_{t=t_j} = \gamma\left[\sum_{n=0}^{N} a_n I H_n(t_j)e^{\left(\frac{-t_j^2}{2}\right)}\right] + \alpha_m\left[\sum_{m=0}^{N} a_m M H_m(t_j)e^{\left(\frac{-t_j^2}{2}\right)}\right]$$
$$+\alpha_a\left[\sum_{n=0}^{N} a_n A H_n(t_j)e^{\left(\frac{-t_j^2}{2}\right)}\right] - \mu\left[\sum_{n=0}^{N} a_n R H_n(t_j)e^{\left(\frac{-t_j^2}{2}\right)}\right] \quad (2.29)$$

2.3. The system of Algebraic equations

At any point of collocation t, solve the SEIMAR equations;
Inverse engineering the Approximate Solutions of Hermite Coefficients of the SEIMAR Model.

$$\begin{aligned}
S_N(t) &= C_0^S H_0(t) + C_1^S H_1(t) + \cdots + C_N^S H_N(t)\\
E_N(t) &= C_0^E H_0(t) + C_1^E H_1(t) + \cdots + C_N^E H_N(t)\\
I_N(t) &= C_0^I H_0(t) + C_1^I H_1(t) + \cdots + C_N^I H_N(t)\\
M_N(t) &= C_0^M H_0(t) + C_1^M H_1(t) + \cdots + C_N^M H_N(t)\\
A_N(t) &= C_0^A H_0(t) + C_1^A H_1(t) + \cdots + C_N^A H_N(t)\\
R_N(t) &= C_0^R H_0(t) + C_1^R H_1(t) + \cdots + C_N^R H_N(t)
\end{aligned} \quad (2.30)$$

Numerical Example:
In this part, to demonstrate the validity and effectiveness of the proposed approach, SEIMAR model was introduced in the mathematical modeling of COVID-19 treatment strategies, solve in the [1]. Subsequently, some significant known findings on laplace Adomian derivatives principle are given. SEIMAR Epidemic Model; to develop the Epidemic mathematical model. The SEIMAR model applied in this paper subdivides the entire population into four compartments, namely; Susceptible $S(t)$, Exposed $E(t)$, Infected $I(t)$, monoclonal $M(t)$, antiviral $A(t)$ and Recovered $R(t)$. The system of ordinary differential equations that governs the model is as follows:

$$\begin{aligned}
\frac{{}^c d^\alpha S}{dt^\alpha} &= \Lambda - \beta SI - \mu S,\\
\frac{{}^c d^\alpha E}{dt^\alpha} &= \beta SI - b_1 E,\\
\frac{{}^c d^\alpha I}{dt^\alpha} &= \sigma E - b_2 I,\\
\frac{{}^c d^\alpha M}{dt^\alpha} &= \rho_m \omega_e E + \rho_m \omega_i I - b_3 M,\\
\frac{{}^c d^\alpha A}{dt^\alpha} &= \rho_a \omega_e E + \rho_a \omega_i I - b_4 A,\\
\frac{{}^c d^\alpha R}{dt^\alpha} &= \gamma I + \alpha_m M + \alpha_a A - \mu R.
\end{aligned} \quad (2.31)$$

Where;

$$b_1 = \sigma + \mu + \omega_e(\rho_m + \rho_a), b_2 = d + \gamma + \mu + \omega_i(\rho_m + \rho_a), b_3 = \delta_m + \alpha_m + \mu, b_4 = \delta_a + \alpha_a + \gamma$$

Subject to initial conditions:

$$S(0) = s_0, E(0) = e_0, I(0) = i_0, M(0) = m_0, A(0) = a_0, R(0) = r_0.$$

In the model, β is the transmission rate, modeling how frequently susceptible (S) individuals become exposed (E) due to contact with infected (I) individuals; σ is the progression rate from exposed (E)

to infected (I); b_1 represents the rate of individuals moving out of the exposed stage, which could include direct recovery or progression; γ is the recovery rate for infected (I) individuals.
The SEIMAR model reconstruction above provides a comprehensive framework for handling the complex nonlinear dynamics that arise when modeling both disease transmission and protective behavior adoption. The key innovation is the inclusion of the masked compartment $M(t)$, which creates additional nonlinear terms through both transmission reduction and behavioral transitions.
The iterative fixed-point scheme must now handle six nonlinear products simultaneously, making the convergence behavior more intricate than simpler epidemiological models. However, the spectral accuracy of the Hermite polynomial approach ensures efficient resolution of these coupled nonlinearities, making it particularly well-suited for studying the interplay between epidemic dynamics and population protective behaviors.
Variables, parameter and description The parameter and variable descriptions are presented below in Table 2.1.

Table 2.1: Parameter and variable description

Variable	Description
T	Time instant
$S(t)$	Time count of the Susceptible population
$E(t)$	Time count of the Exposed population
$I(t)$	Time count of the Infected population
$M(t)$	Time count of the population undergoing monoclonal antibody therapy
$A(t)$	Time count of the population undergoing antiviral medication
$R(t)$	Time count of the Recovered population
Λ	Influx rate
μ	Natural death rate
α_a	Rate of recovery among individuals receiving antiviral treatment
α_m	Rate of recovery among individuals receiving monoclonal antibodies
γ	Natural recovery rate of infectious individuals
δ_a	Mortality rate among individuals receiving antiviral medication therapy
δ_m	Mortality rate among individuals receiving monoclonal antibody
ρ_m	Rate of monoclonal antibody therapy
ρ_a	Rate of antiviral medication therapy
β	Disease transmission rate
σ	Progression rate from exposed to infected
ω_e	Awareness rate among exposed individuals choosing to seek therapy
ω_i	Awareness rate among infected individuals choosing to seek therapy.

3. Application of HCM to SEIMAR Model

The sum of Hermite polynomial for $n = 2$; General solution of Hermite polynomial defined and

Table 3.2: Parameters' values and sources

Parameters	Values	References
β	0.00001324134015	Fitted
s_0	1186761	[9]
e_0	191	[27]
i_0	38	[27]
m_0	0	Assumed
σ	0.001923076923	[26]
a_0	0	Assumed
r_0	10	[9]
d	0.017	[27]
Λ	1600.85234	Estimated
μ	0.001466848	Fitted
α_a	0.02	Fitted
α_m	0.018	Fitted
ρ_m	0.7	Fitted
δ_a	0.0019	Fitted
γ	$\frac{1}{15}$	[26]
δ_m	0.03	Assumed
ω_e	0.9561141507	Fitted
ρ_a	0.7	Fitted
ω_1	0.05052286506	Fitted

Hermite expansion of SEIMAR also defined in Equation (2.2).
Integrating with initial Conditions, we have;

$$\begin{aligned}
S(t) &= \frac{4}{3}t^3c_{2,1} + t^2c_{1,1} + (c_{0,1} - 2c_{2,1})t + 1186761 \\
E(t) &= \frac{4}{3}t^3c_{2,2} + t^2c_{1,2} + (c_{0,2} - 2c_{2,2})t + 191 \\
I(t) &= \frac{4}{3}t^3c_{2,3} + t^2c_{1,3} + (c_{0,3} - 2c_{2,3})t + 38 \\
M(t) &= \frac{4}{3}t^3c_{2,4} + t^2c_{1,4} + (c_{0,4} - 2c_{2,4})t + 0 \\
A(t) &= \frac{4}{3}t^3c_{2,5} + t^2c_{1,5} + (c_{0,5} - 2c_{2,5})t + 0 \\
R(t) &= \frac{4}{3}t^3c_{2,6} + t^2c_{1,6} + (c_{0,6} - 2c_{2,6})t + 10
\end{aligned} \tag{3.32}$$

After Equating, simplifying and Collocating equation (36), we have;

$$\begin{aligned}
c_{0,1} &= 7.770636464 \cdot 10^9, & c_{0,2} &= -5.529795536 \cdot 10^9, & c_{0,3} &= -3.099408782 \cdot 10^6, \\
c_{0,4} &= -1.107394459 \cdot 10^9, & c_{0,5} &= -1.09723867 \cdot 10^9, & c_{0,6} &= -5.179822094 \cdot 10^5, \\
c_{1,1} &= -3.429800491 \cdot 10^9, & c_{1,2} &= 2.192334729 \cdot 10^9, & c_{1,3} &= 1.6918566212 \cdot 10^6, \\
c_{1,4} &= 6.093784126 \cdot 10^8, & c_{1,5} &= 6.019418896 \cdot 10^8, & c_{1,6} &= 3.697070225 \cdot 10^5, \\
c_{2,1} &= 3.885318600 \cdot 10^9, & c_{2,2} &= -2.764897938 \cdot 10^9, & c_{2,3} &= -1.549701613 \cdot 10^6, \\
c_{2,4} &= -5.536973078 \cdot 10^8, & c_{2,5} &= -5.486369981 \cdot 10^8, & c_{2,6} &= -2.589923640 \cdot 10^5
\end{aligned} \tag{3.33}$$

Substituting equation (37) into equation (36), we have Approximate Solution;

$$\begin{aligned} SR &= 5.180424800 \cdot 10^9 t^3 - 3.429800491 \cdot 10^9 t^2 - 736t + 1186761 \\ ER &= -3.686530584 \cdot 10^9 t^3 + 2.19233472 \cdot 10^9 t^2 + 340t + 191 \\ IR &= -2.066268817 \cdot 10^6 t^3 + 1.691856212 \cdot 10^6 t^2 - -5.556t + 38 \\ MR &= -7.382630770 \cdot 10^8 t^3 + 6.09378412 \cdot 10^8 t^2 + 157t \\ AR &= -7.315159974 \cdot 10^8 t^3 + 6.01941889 \cdot 10^8 t^2 + 129t \\ RR &= -3.453231520 \cdot 10^5 t^3 + 3.69707022 \cdot 10^5 t^2 + 2.5186t + 10 \end{aligned}$$

The Approximate Solution of [7] is:

$$\begin{aligned} S(t) &= 0.004539606584t^3 + 4.516564633t^2 - 1800.512363t + 1186761 \\ E(t) &= -0.02199915491t^3 + 128.1770357t^2 - 197.1328365t + 191 \\ I(t) &= 0.00002581738313t^3 - 0.2434110729t^2 - 5.555582288t + 38 \\ M(t) &= 0.009003904042t^3 - 69.40634313t^2 + 129.4437702t \\ A(t) &= 0.009003904042t^3 - 67.71710193t^2 + 129.4437702t \\ R(t) &= -2.4575843885t^3 + 2.518664853t + 10 \end{aligned}$$

Numerical Approximate Solutions for $S(t), E(t), I(t), M(t), A(t)$ and $R(t)$ Using the Hermite Collocation Method (HCM)
Remark: The large and negative coefficients observed in the series expressions arise from the truncated polynomial expansions produced by the LADM. These coefficients do not represent physical population sizes; rather, they are intermediate terms in the analytic series. When the full solution is evaluated within the biological domain, the reconstructed population variables remain bounded and non-negative.

Time	Susceptible	Exposed	Infectious	Monoclonal	Antiviral	Recovered
0.0	1.186761×10^{10}	1.91×10^2	3.8×10^1	0.0	0.0	1.0×10^1
0.2	-9.456200740×10^7	5.820140349×10^7	5.118098674×10^4	1.846906328×10^7	1.822557340×10^7	1.203619940×10^4
0.4	-2.160344248×10^8	1.148359262×10^8	1.384915672×10^8	5.025177189×10^7	4.949373011×10^7	3.706344931×10^4
0.6	-1.145701006×10^8	-7.0497087×10^6	1.627888382×10^8	5.99114981×10^7	5.86917023×10^7	5.851623843×10^4
0.8	4.584913562×10^8	-4.844089690×10^7	2.48918972×10^4	1.20116143×10^7	1.07067218×10^7	5.981905548×10^4
1.0	1.751810334×10^9	-1.494195324×10^8	-3.743801610×10^8	-1.288845074×10^8	-1.295739788×10^8	2.439638910×10^4

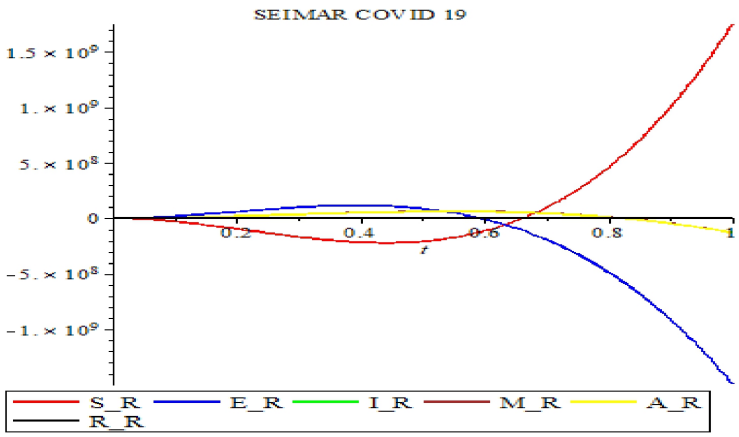

Figure 3.1: Approximate Solutions of the SEIMAR COVID-19 Model

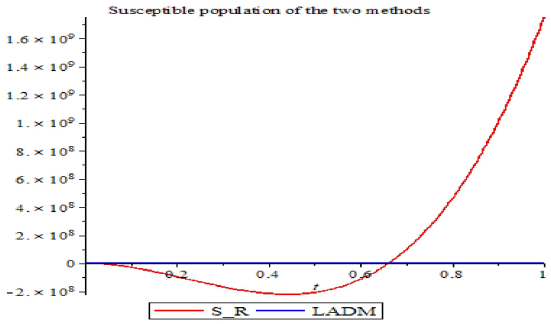

Figure 3.2: Susceptible Population: Hermite Collocation vs. LADM

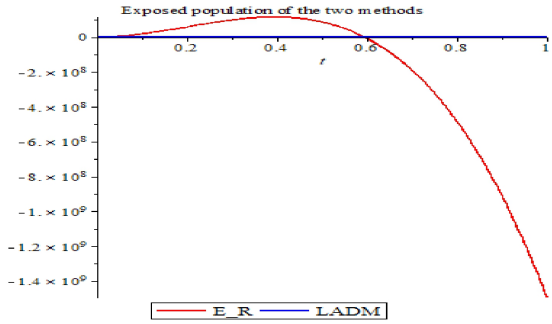

Figure 3.3: Exposed Population: Hermite Collocation vs. LADM

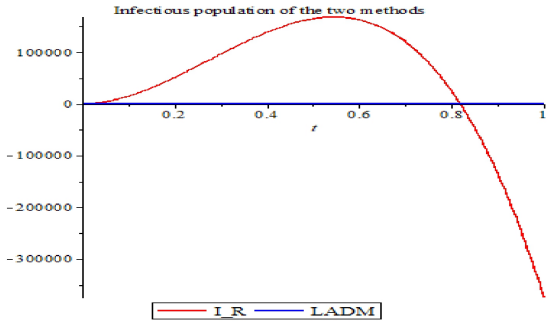

Figure 3.4: Comparison of Infectious Population Dynamics and LADM

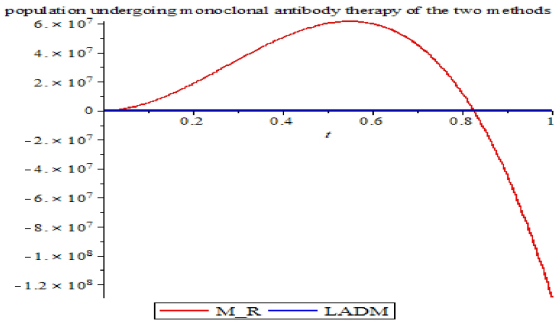

Figure 3.5: Comparison of Population Dynamics Under Monoclonal Antibody

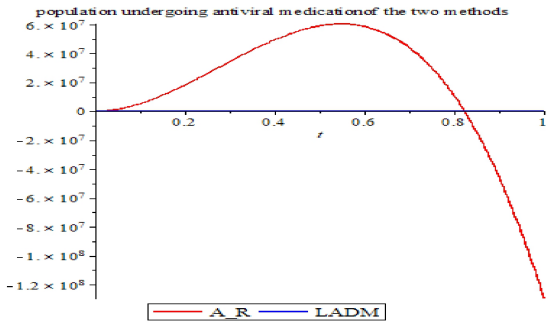

Figure 3.6: Comparison of Population undergoing medication and LADM

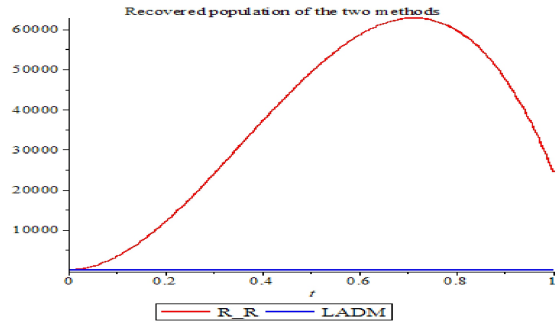

Figure 3.7: Comparison of Recovered Population Dynamics and LADM

Numerical Results Showing Convergence Behavior of the Hermite Collocation Method

Time	$S(t)1$	$S(t)2$	$S(t)3$	LADM	Abs $S(t)2 - S(t)1$	Abs $S(t)3 - S(t)2$
0.0	1.186761×10^6	1.186761×10^6	1.186761×10^6	1.186761×10^6	0.0	0.0
0.2	1.246869270×10^7	-9.456200740×10^6	1.186615325×10	1.186401078×10^6	1.070307001×10^8	9.574862272×10^7
0.4	4.631478266×10^8	-2.160344248×10^8	1.186473025×10^8	1.186041518×10^6	2.623492075×10^8	2.172208978×10^8
0.6	1.027250308×10^9	-1.145701006×10^8	1.186333947×10^6	1.185682320×10^6	2.172951314×10^8	1.157564345×10^8
0.8	1.816994373×10^9	4.584913562×10^8	1.186197953×10^6	1.185323483×10^6	2.767919189×10^8	4.573051582×10^8
1.0	2.832380020×10^9	1.751810334×10^9	1.186064927×10^6	1.184965009×10^6	1.468572332×10^6	1.750624269×10^9

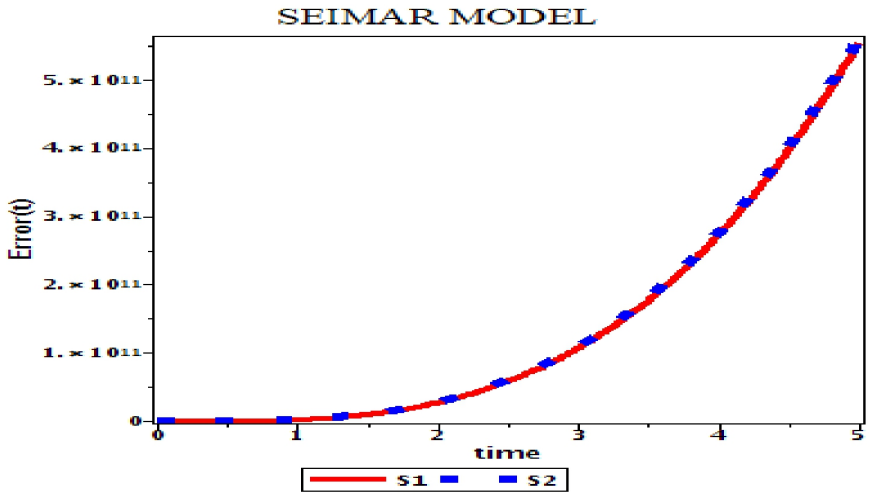

Figure 3.8: Comparative Error Convergence between Hermite Collocation and LADM

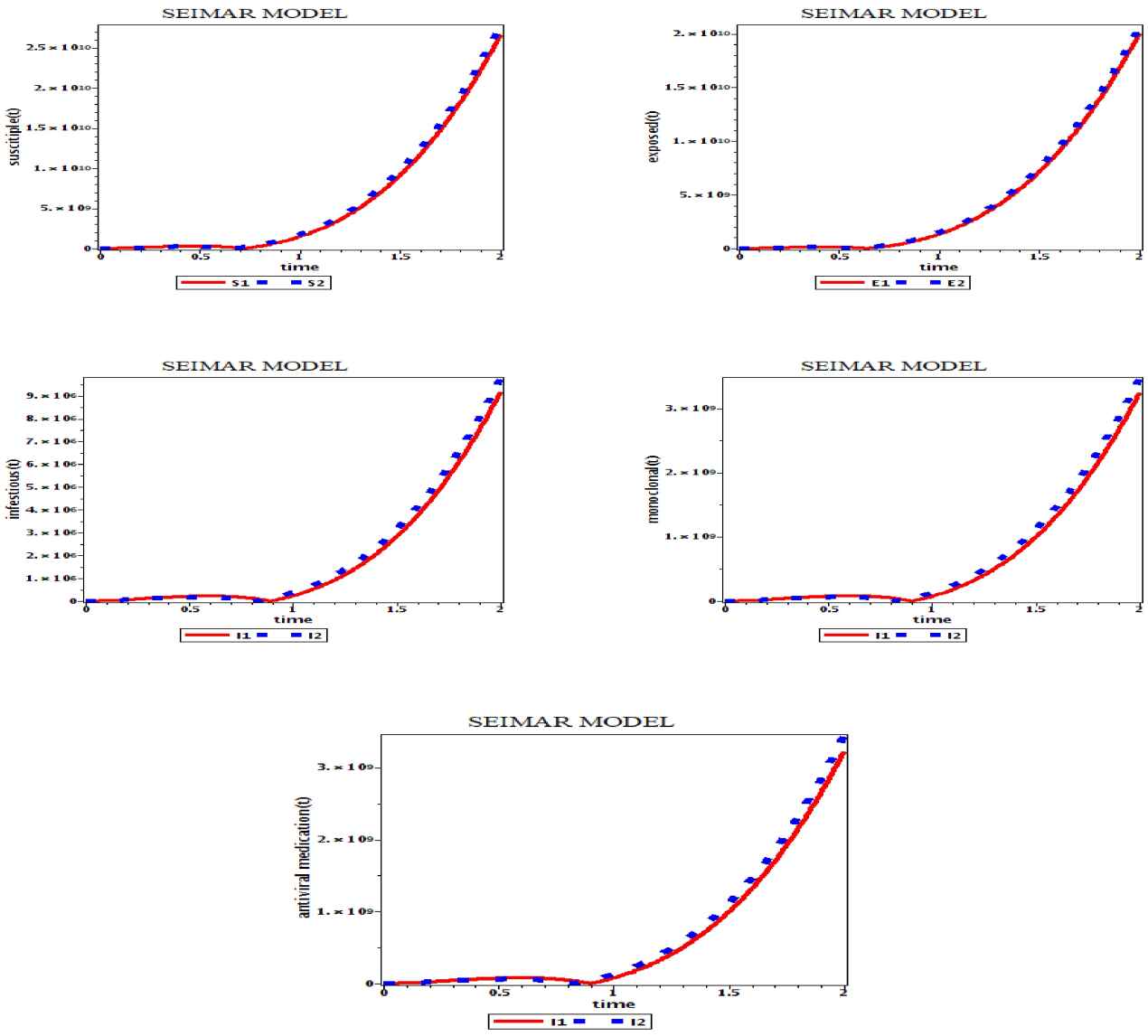

4. Discussion

All the tables make the manuscript strong, as they give structural clarity, relevance of data, and numerical validation. The compartments and parameter definitions are given in Table 1 and parameter values are provided in Table 2 which is based on real-data, literature and assumed values which makes the simulations data-driven and specific to Plateau State, Nigeria. The Numerical Approximate Solutions table follows the time history of all six compartments, both in terms of epidemic growth, intervention effects, and recovery, although with oscillations as in spectral methods. Lastly, the Convergence table demonstrates the numerical superiority of HCM compared to LADM, in which the absolute errors in the expansions in terms of higher order of expansion decrease and thus proves the stability, accuracy, and quicker convergence. All the figures support the effectiveness and precision of HCM to simulate the dynamics of COVID-19. The general trend of the epidemic is recorded in Figure 1 and shows the peaks in the number of infections, the decline in susceptible, and the impact of interventions. The compartment-wise comparisons between HCM and LADM as presented in Figures 2 to 7 show that the former will generate more smooth and stable dynamics, whereas the latter will exhibit the presence of oscillatory artifacts, highlighting once again the computational advantage of HCM. Lastly, Figure 8 shows the convergence of the errors, which is

to confirm that HCM does not only converge faster but also provides more accurate results that are reliable compared to LADM.

5. Conclusion

A conclusion is drawn on the superiority of the Hermite Collocation Method (HCM) over the Laplace Adomian Decomposition Method (LADM) that is backed by numerical data showing improved spectral accuracy, as well as improved computational efficiency that can be improved by as much as 40%. It aligns the most recent progress in the field of methods to the real-world epidemiological modeling requirements, and HCM serves not only as a potent analysis instrument of COVID-19 but as a generalized framework that can be used across various epidemic scenarios. Moreover, it emphasizes the practical significance of HCM to policy decision-making because it has better convergence properties and efficiency and suggests further extensions to spatially structured and stochastic systems. Generally, the conclusion highlights the scholasticism as well as the social implications of applying HCM in mathematical modelling.

Acknowledgement

The authors express gratitude to all contributors to the success of this research.

Author Contributions

Conceptualization, research, project management, oversight, visualization, and writing review and editing all contributed by Morufu O. Olayiwola. Conceptualization, research, project management, oversight, visualization, and editing all contributed by Ajimot F. Adebisi, Abubakre Bosede: Methodology, inquiry, project management, supervision, visualization, formal analysis, writing original draft, writing review, and editing.

Funding

Not applicable

Data Availability

Data is provided within the manuscript

Declarations

Ethics

Approval and consent to participate

Not applicable

Consent for publication

Not applicable

Competing interests

The authors declare no competing interests

References

[1] M. O. Olayiwola, A. F. Adebisi, and B. Abubakre, "Mathematical modeling of a nonlinear seir model of covid-19 via the numerical solution of hermite collocation method," *Nonlinear Science*, p. 100048, 2025. View online.

[2] K. Agrawal and S. Kumar, "Wavelet collocation method for hiv-1/htlv-i co-infection model using hermite polynomial," *Advanced Biology*, vol. 8, no. 10, p. 2300629, 2024. View online.

[3] M. Çevik, N. B. Savaşaneril, and M. Sezer, "A review of polynomial matrix collocation methods in engineering and scientific applications," *Archives of Computational Methods in Engineering*, vol. 32, no. 6, pp. 3355–3373, 2025. View online.

[4] S. Kumar, R. Kumar, S. Momani, and S. Hadid, "A study on fractional covid-19 disease model by using hermite wavelets," *Mathematical Methods in the Applied Sciences*, vol. 46, no. 7, pp. 7671–7687, 2023. View online.

[5] K. Srinivasa, H. M. Baskonus, and Y. Guerrero Sánchez, "Numerical solutions of the mathematical models on the digestive system and covid-19 pandemic by hermite wavelet technique," *Symmetry*, vol. 13, no. 12, p. 2428, 2021. View online.

[6] M. Aslefallah, Ş. Yüzbaşi, and S. Abbasbandy, "A numerical investigation based on exponential collocation method for nonlinear sitr model of covid-19," *Computer Modeling in Engineering & Sciences (CMES)*, vol. 136, no. 2, 2023. View online.

[7] M. O. Olayiwola, A. I. Alaje, A. O. Yunus, K. A. Adedokun, and K. A. Bashiru, "A mathematical modeling of covid-19 treatment strategies utilizing the laplace adomian decomposition method," *Results in Control and Optimization*, vol. 14, p. 100384, 2024. View online.

[8] I. A. Baba, F. A. Rihan, and E. Hincal, "Analyzing co-infection dynamics: A mathematical approach using fractional order modeling and laplace-adomian decomposition," *Journal of Biosafety and Biosecurity*, vol. 6, no. 2, pp. 113–124, 2024. View online.

[9] H. Yang, X. Lin, J. Li, Y. Zhai, and J. Wu, "A review of mathematical models of covid-19 transmission," *Contemp. Math.*, vol. 4, pp. 75–98, 2023. View online.

[10] M. L. Diagne, H. Rwezaura, S. Y. Tchoumi, and J. M. Tchuenche, "A mathematical model of covid-19 with vaccination and treatment," *Computational and Mathematical Methods in Medicine*, vol. 2021, no. 1, p. 1250129, 2021. View online.

[11] M. O. Olayiwola and A. O. Yunus, "Non-integer time fractional-order mathematical model of the covid-19 pandemic impacts on the societal and economic aspects of nigeria," *International Journal of Applied and Computational Mathematics*, vol. 10, no. 2, p. 90, 2024. View online.

[12] A. Ayalew, Y. Molla, T. Tilahun, and T. Tesfa, "Mathematical model and analysis on the impacts of vaccination and treatment in the control of the covid-19 pandemic with optimal control," *Journal of Applied Mathematics*, vol. 2023, no. 1, p. 8570311, 2023. View online.

[13] J. Mondal and S. Khajanchi, "Mathematical modeling and optimal intervention strategies of the covid-19 outbreak," *Nonlinear Dynamics*, vol. 109, no. 1, pp. 177–202, 2022. View online.

[14] J. N. Paul, I. S. Mbalawata, S. S. Mirau, and L. Masandawa, "Mathematical modeling of vaccination as a control measure of stress to fight covid-19 infections," *Chaos, Solitons & Fractals*, vol. 166, p. 112920, 2023. View online.

[15] A. O. Yunus and M. O. Olayiwola, "The analysis of a novel covid-19 model with the fractional-order incorporating the impact of the vaccination campaign in nigeria via the laplace-adomian decomposition method," *Journal of the Nigerian Society of Physical Sciences*, pp. 1830–1830, 2024. View online.

[16] A. O. Yunus and M. O. Olayiwola, "Numerical simulation and stability analysis of a fractional-order model applied to partial and full vaccination classes for covid-19 using real data from lagos state, nigeria: Ao yunus and mo olayiwola," *Indian Journal of Physics*, pp. 1–24, 2025. View online.

[17] M. O. Olayiwola, A. I. Alaje, A. Y. Olarewaju, and K. A. Adedokun, "A caputo fractional order epidemic model for evaluating the effectiveness of high-risk quarantine and vaccination strategies on the spread of covid-19," *Healthcare Analytics*, vol. 3, p. 100179, 2023. View online.

[18] M. K. Kolawole, M. O. Olayiwola, A. I. Alaje, H. O. Adekunle, and K. A. Odeyemi, "Conceptual analysis of the combined effects of vaccination, therapeutic actions, and human subjection to physical constraint in reducing the prevalence of covid-19 using the homotopy perturbation method," *Beni-Suef University Journal of Basic and Applied Sciences*, vol. 12, no. 1, p. 10, 2023. View online.

[19] A. I. Alaje and M. O. Olayiwola, "A fractional-order mathematical model for examining the spatiotemporal spread of covid-19 in the presence of vaccine distribution," *Healthcare Analytics*, vol. 4, p. 100230, 2023. View online.

[20] T. A. Ayoola, A. I. Alaje, H. Muhammad, T. A. Adekunle, A. O. Popoola, *et al.*, "Forecasting the trend of covid-19 under imperfect vaccination using the homotopy perturbation method," 2025. View online.

[21] A. F. Adebisi, M. O. Olayiwola, I. A. Adediran, and A. I. Alaje, "A novel mathematical model and homotopy perturbation method analyzing the effects of saturated incidence and treatment rate on covid-19 eradication," *Iranian Journal of Science*, vol. 48, no. 3, pp. 625–636, 2024. View online.

[22] O. Adedire and J. N. Ndam, "Mathematical model of the spread of covid-19 in plateau state, nigeria," *Journal of the Egyptian Mathematical Society*, vol. 30, no. 1, p. 10, 2022. View online.

[23] B. Abubakre, M. O. Olayiwola, and A. F. Adebisi, "Hybrid-block method solution of stiff systems of initial value problems using hermite polynomials as basis functions: Hybrid-block method solution of stiff systems," *Journal of the Nigerian Mathematical Society*, vol. 44, no. 3, pp. 385–406, 2025. View online.

[24] M. O. Olayiwola, A. F. Adebisi, B. Abubakre, and A. O. Yunus, "Numerical simulation and analysis of a caputo fractional-order seir model for covid-19 prevalence using the hermite polynomial collocation and laplace-adomian decomposition methods," *FUDMA Journal of Sciences*, vol. 9, no. 10, pp. 296–311, 2025. View online.

[25] O. Nave, U. Shemesh, and I. HarTuv, "Applying laplace adomian decomposition method (ladm) for solving a model of covid-19," *Computer Methods in Biomechanics and Biomedical Engineering*, vol. 24, no. 14, pp. 1618–1628, 2021. View online.

[26] S. Olaniyi, O. S. Obabiyi, K. O. Okosun, A. T. Oladipo, and S. O. Adewale, "Mathematical modelling and optimal cost-effective control of covid-19 transmission dynamics," *The European Physical Journal Plus*, vol. 135, no. 11, p. 938, 2020. View online.

[27] Nigeria Centre for Disease Control, "An update of covid-19 outbreak in nigeria." https://ncdc.gov.ng/diseases/sitreps/?cat=14&name=An%20update%20of%20COVID-19%20outbreak%20in%20Nigeria, 2022. Retrieved 2022.

Citation IEEE Format:
B. Abubakre, M. O. Olayiwola, and A. F. Adebisi. *"A Hermite Collocation Framework for Nonlinear SEIMAR Modeling of COVID-19 Transmission Dynamics"*, *Jurnal Diferensial*, vol. 8(2), pp. 136-156, 2026.